Applied Thermal Engineering 143 (2018) 812–821

Contents lists available at ScienceDirect

Applied Thermal Engineering

journal homepage: www.elsevier.com/locate/apthermeng

Research Paper

Energy optimal control of thermal comfort in trams

Raphael N. Hofstadter[a,*], Jorge Amaya[b], Martin Kozek[a]

[a] Vienna University of Technology, Institute of Mechanics and Mechatronics, Vienna, Austria
[b] Universidad de Chile, Center for Mathematical Modeling, Santiago, Chile

HIGHLIGHTS

- Provides an insight of the implementation to a rapid controller prototyping platform.
- Shows and discusses the measured results from climatic wind tunnel experiments.
- Achieves an annual energy saving of 32% for the entire temperature range.

ABSTRACT

This paper presents a method for thermal comfort control for trams which achieves the desired thermal comfort and minimises the power consumption of heating, ventilation and air conditioning (HVAC). Mathematical models of all relevant parts are stated (these parts being the tram and the HVAC considering both comfort and energy consumption) and these models are linearised.

Using linearised models, cascaded control loops are established. A model-predictive controller regulates the thermal comfort inside the tram as a master controller and outputs an auxiliary control variable to the slave controller. A heuristic, realised as mixed-integer optimisation, converts the auxiliary control variable in an energy-optimal way into switching commands for the HVAC. For validation, the method is implemented on a rapid controller prototyping platform. Testing of the control approach is done during several climatic wind tunnel measurements. The annual energy consumption is extrapolated using these results.

1. Introduction

Already in 1990, the Intergovernmental Panel on Climate Change announced that emissions resulting from humans would enhance the natural greenhouse effect, resulting on average in an extra warming of the Earth's surface [1]. The European Union thus follows the objective of increasing energy efficiency of products and services [2].

Energy efficiency of transport is important for the overall energy consumption. Many German researchers point out that transportation consumes 30% of the final energy consumption [3]. The modal split specifies (in percent) which means of transport travellers use. Percentages for public transport range from (almost) 0 to 60%, depending on the region. Even though railway transport is already more energy efficient than other means of transport [4] and its efficiency was increased significantly in the past decade [5], a further increase is still possible. Researchers achieved many energy-saving measures for propulsion in the past years, by consistent lightweight design [6], driver assistance systems and hybridisation [7], for example.

Struckl [8] showed energy saving potential for rail vehicles using Oslo's subway as an example. HVACs consume about 30% of the total energy during driving cycles [8, see Figure 4.53]. So, they are the second largest energy consumer. Later research confirmed this extent.

One approach to increase the energy efficiency of HVACs is to improve the ventilation efficiency. Air displacement ventilation can achieve this. Researchers have already used it successfully in buildings, aeroplanes [9] and recently in rail vehicles, too [10].

Another approach is to increase the energy efficiency of the heating, ventilation and air conditioning (HVAC) unit itself. Energy-saving measures known from other HVAC applications also apply to rail vehicles, such as demand-based ventilation, heating by a heat pump, variable frequency drive of the compressor and fine-grained control of the electric heater. These measures allow the HVAC unit to closely follow the demand, but with extra parts and fine-grained control, the complexity of the control problem rises. Model predictive control (MPC, also known as receding horizon control, rolling horizon planning and dynamic programming) is a proven method of control. The control action at each time step is obtained by solving an optimisation problem for the given time horizon. The resulting optimisation problem can often be formulated as a quadratic program [11] with real decision variables. Combinatorial optimization problems can sometimes be solved by (mixed) integer linear programming (MILP), which seeks the best result from a finite set of solutions is sought. Decision variables can

* Corresponding author.
E-mail address: r.hofstaedter@gmail.com (R.N. Hofstadter).

https://doi.org/10.1016/j.applthermaleng.2018.07.084
Received 17 December 2017; Received in revised form 4 June 2018; Accepted 16 July 2018
Available online 01 August 2018
1359-4311/

Nomenclature

List of Subscripts and Superscripts

AAC	after air condition
ac	air condition
air	air
comp	compressor
down	rounded down to the nearest integer
eh	electrical heater
est	estimated
EXH	exhaust air
fan	fan
hp	heat pump
IDA	indoor air
loss	losses from the vehicle to the environment
lb	lower bound of …
~	augmented …
mc	mixing chamber
ODA	outdoor air
pas	passengers
pas,CO2	CO2 amount of passengers
pas,sen	sensible heat of passengers
ref	reference
sol	solar radiation
SUP	supply air
tot	total
ub	upper bound of …
up	rounded up to the nearest integer
vapour	vapour
veh	vehicle

List of Symbols

$\mathbf{A}$	state (or system) matrix of the state space system
$\mathbf{B}$	input matrix of the state space system
$\mathscr{B}$	heating (el + CRM) mode
β	AAC ratio
C	heat capacity
$\mathbf{C}$	output matrix of the state space system
$\mathscr{C}$	cooling mode
c	specific heat capacity
$\mathbf{D}$	feedthrough (or feedforward) matrix of the state space system
$\mathscr{D}$	dehumidification mode
$\dot{E}$	Enthalpy flow
$\mathbf{E}$	disturbance matrix of the state space system
$\mathscr{E}$	heating (el) mode
e	control error
f	coefficient or scaling factor
g	constraints vector of the MPC problem
$\mathbf{G_1}$	constraints matrix of the state vector of the MPC problem
$\mathbf{G_2}$	constraints matrix of the control vector of the MPC problem
$\mathscr{H}$	Heating (CRM) mode
Δh_{SUP}	the control variable of the MPC problem, effects the temperature
Δh_V	evaporation heat of water
$\mathbf{I}$	identity matrix
i	index of the before calculated solutions
J	objective function
k	heat transfer coefficient
$\mathscr{M}$	HVAC mode
m	mass
$\dot{m}$	mass flow
n	number of …
O	uncoiled surface of the vehicle
P	electric power consumption
$\mathscr{P}$	a point in the diagram
φ	discrete control variable of the HVAC
$\mathbf{Q}$	weighting matrix for the control error
$\dot{Q}$	heat flow
$\dot{q}_{sol}$	power of solar radiation
$\mathbf{R}$	weighting matrix for the control vector
ρ	density
σ	carbon dioxide concentration
$\Delta\sigma_{SUP}$	the control variable of the MPC problem, effects the CO2 concentration
T	temperature
t	continuous time
τ	control horizon
ϑ	discrete time
u	control vector of the state space system
Δu	change of the control variable
u_{HVAC}	control vector of the HVAC
V	volume
$\mathscr{V}$	ventilating mode
v	disturbance vector of the state space system
w	reference vector
x	state vector of the state space system
Y	absolute humidity of air
y	output vector of the state space system

be real, integer, binary or a combination thereof. Hybrid systems have both continuous and discrete dynamic behaviour. A vapour-compression refrigeration system can be described as a hybrid system, for example. In [12] modelling and optimal control of supermarket refrigeration systems are presented. Elliott et al. [13] use cascaded control for a multi-evaporator vapour compression cooling cycle, in which they set up the outer controller as a model predictive controller (MPC). Bejarano et al. [14] use a suboptimal hierarchical control strategy to improve the energy efficiency of vapour-compression refrigeration systems. Also, [15] uses a binary variable (on-off) for temperature control in refrigerated transport systems. The authors of [16] introduce a distributed model predictive control scheme for supermarket refrigeration systems and [17] takes daily variations of i.a. electricity prices into account. Hybrid systems sometimes describe the building heating control problem, in which, for example, a mixed integer MPC is used for the integer variables as in [18,19]. Hybrid systems and their control also occur in energy management [20] and powertrains of (hybrid) vehicles [21].

The trend for improving thermal comfort and reducing the necessary energy consumption is set by the automotive industry. Muhammad et al. [22] studied the influence of thermostat level setting on fuel consumption and thermal comfort for the passenger compartment of a car. A new personal thermal comfort model is developed by Kim et al. [23] predicting an individual's thermal comfort response instead of the average response of a large population. Mathematical models and their validation for thermal comfort, air quality, and energy use are proposed by Kristanto et al. [24] for a car cabin. Since thermal comfort in the car influences the buying decision in the automotive industry, all concerns of this comfort are examined in detail. Bode et al. [25] researched the influence of the inlet angle of an air diffuser on the thermal comfort of passengers in a car. Velivelli et al. [26] examined the seat cooling distribution to further improve human thermal comfort in automotive

environments.

In contrast to all the cited references, the work presented here contains the following unique contributions: A summary of thermodynamic models for a tram and an HVAC is presented; a controller design taking thermal comfort and energy consumption into account is proposed. The controller is implemented on to a rapid controller prototyping platform (RCPP) and tested during a measuring campaign in the Viennese climatic wind tunnel (CWT).

The objective of this work is to describe the control problem of thermal comfort in rail vehicles and solve it by using as little electrical energy for the HVACs as possible. Models for the entire thermal comfort problem in rail vehicles are derived (tram, HVAC, thermal comfort). Two different approaches for its control are presented. First, the overall control problem is split into two sub-problems to facilitate calculation. A model predictive controller controls the thermal comfort inside the train by writing out auxiliary control variables. An integer linear optimisation converts these auxiliary controls in an energy-optimal way into switching commands for the HVAC. Second, the control problem is simplified by ruling out unwanted switching commands, and a method based on MPC is used to solve it.

Algorithms and the needed software libraries are compiled for an RCPP, which is built into the tram. Results from a twelve-day measuring campaign in the CWT show that it is possible to maintain thermal passenger comfort and reduce the energy consumption of the HVAC.

Section 2 studies the thermal behaviour of a tram, prepares and linearises its analytical model.Section 3 describes the control loop and designs the master and the slave controller in addition, it provides an insight of the controller implementation on to a rapid controller prototyping platform is provided.Section 4 shows and discusses the measured results from CWT. In the end,Section 5 summarises main results and shows potential for further research.

2. Modelling

The studied rail vehicle is the Ultra Low Floor tram A1, made by Siemens AG Österreich and managed by the Wiener Linien GmbH & Co KG in Vienna. The tram is about 24 m long, 2.4 m wide and 3 m high with an unloaded weight of 30 t. It is split into three similar sections with an added bow and tail section. Fig. 1 shows a schematic of the tram. There are twelve seats in every section, five more seats in the tail section and a wheelchair space in the bow; resulting in 42 seats total. Also, there is space for 94 standing passengers.

All three main sections of the tram contain their own HVAC unit. Each HVAC can heat, ventilate, cool and dehumidify the tram. The Vossloh-Kiepe GmbH designed the HVACs, especially for a high energy efficiency.

Train, HVAC and controller form a closed control loop of climiatization. In the train a specific state (that is a temperature) of indoor air exists, also called actual value. Various sensors (that are thermocouples) make measurements and send them to the controller. The controller produces a control error from comparing set-points and measurements. Then, the controller calculates a control signal and sends it to the HVAC. The HVAC properly conditions the supply airflow to the train to minimize the control error. This conditioning of air needs electrical energy. Various disturbances act on the train and on the HVACs and so the indoor air reaches a new state.

2.1. Train

Relevant variables for thermal comfort inside the train are the temperature of the indoor air and humidity according to current standards [27,28]. This approach adds carbon dioxide concentration to allow demand-based ventilation.

It needs a dynamic train model to describe the indoor air temperature T_{IDA} and the carbon dioxide concentration of indoor air σ_{IDA}. Humidity is also an important variable, but the approach presented here does not contain a closed-loop control for humidity is implemented. The local weather justifies this because it is favourable in this regard.

The authors of [29] use an analytical approach is used to develop a thermodynamic model of a train. They use the same approach to simulate the energy consumptions of HVACs [30]. A similar approach was used for calculating values of heat transfer coefficients and heat capacities for various rail vehicle classes in [31]. Thermodynamics as described in [29,31] form the basis of this work.

2.1.1. Overall train model

The authors of [31] assume the train consists of two thermal systems with two heat capacities and two temperatures (the indoor air temperature T_{IDA} and a fictitious temperature T_{veh} of the train's heat capacity). The two non-stationary energy balances for a section of the train are

$$C_{IDA}\frac{dT_{IDA}}{dt} = -\dot{Q}_{loss} - \dot{Q}_{veh} + \dot{Q}_{sol} + \dot{Q}_{pas} + \dot{E}_{SUP} - \dot{E}_{EXH} \tag{1a}$$

$$C_{veh}\frac{dT_{veh}}{dt} = \dot{Q}_{veh} \tag{1b}$$

where C_{IDA} is the heat capacity associated with temperature T_{IDA}. $\dot{Q}_{loss} = k_{IDA}(t)\cdot O\cdot(T_{ODA} - T_{IDA})$ describes the dissipated heat from the train (temperature T_{IDA}) to the environment (or the outdoor air temperature T_{ODA}). $k_{IDA}(t)$ is the train's heat transfer coefficient and O is the uncoiled surface of the train. $\dot{Q}_{veh} = k_{veh}\cdot(T_{IDA} - T_{veh})$ is the energy flow between the two thermal systems with temperatures T_{IDA} and T_{veh}, respectively. k_{veh} is the fictitious heat transfer coefficient between these systems and C_{veh} is the heat capacity associated with temperature T_{veh}. Note that C_{veh} is a ficticious average heat capacity lumping together all masses in thermal interaction with the indoor air. $\dot{Q}_{sol} = k_{sol}(t)\cdot\dot{q}_{sol}$ considers the solar radiation (direct and indirect), in which $k_{sol}(t)$ is the absorption coefficient and $\dot{q}_{sol}$ is the power of the solar radiation. $\dot{Q}_{pas} = k_{pas}(t)\cdot n_{pas}$ considers the dissipated sensible heat by passengers, in which $k_{pas}(t)$ is the amount of dissipated heat per passenger and n_{pas} is the number of passengers. $\dot{E}_{SUP} = \dot{m}_{SUP}\cdot c_{air}\cdot T_{SUP}$ is the enthalpy flow of supply air and $\dot{E}_{EXH} = \dot{m}_{SUP}\cdot c_{air}\cdot T_{IDA}$the enthalpy flow of exhaust air. $\dot{m}_{SUP}$ is the mass flow of supply air, c_{air} its specific heat capacity and T_{SUP} the supply air temperature. So, $\dot{m}_{SUP}\cdot c_{air}\cdot(T_{SUP} - T_{IDA})$ contains the enthalpy change inside the train because of the HVAC. Fig. 2 shows heat and mass flows for a section of the train. Eq. (1) can be rewritten by inserting the following for the right-hand side terms [see also 29,31]:

$$C_{IDA}\cdot\frac{dT_{IDA}}{dt} = k_{IDA}(t)\cdot O\cdot(T_{ODA} - T_{IDA}) - k_{veh}\cdot(T_{IDA} - T_{veh}) + \dot{m}_{SUP}\cdot c_{air}\cdot(T_{SUP} - T_{IDA}) + k_{pas}(t)\cdot n_{pas} + k_{sol}(t)\cdot\dot{q}_{sol} \tag{2a}$$

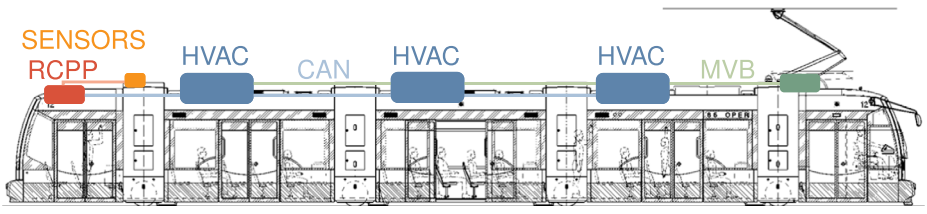

Fig. 1. Schematic of the tram.

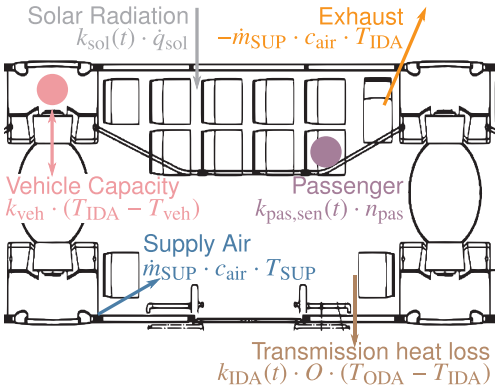

Fig. 2. Schematic of heat and mass flows for train section that contains its own HVAC.

$$C_{veh} \cdot \frac{dT_{veh}}{dt} = k_{veh} \cdot (T_{IDA} - T_{veh}). \tag{2b}$$

$$V_{IDA} \cdot \rho_{IDA} \cdot \frac{d\sigma_{IDA}}{dt} = \dot{m}_{SUP} \cdot (\sigma_{SUP} - \sigma_{IDA}) + + f_{pas} \cdot n_{pas}. \tag{3}$$

Eq. (3) allows calculating the carbon dioxide concentration inside the train σ_{IDA}, in which V_{IDA} is the indoor air volume and ρ_{IDA} is its density. The carbon dioxide amount removed by the supply air is $\dot{m}_{SUP} \cdot (\sigma_{SUP} - \sigma_{IDA})$. σ_{SUP} is the carbon dioxide concentration of the supply air. Passengers give off carbon dioxide while breathing, it is $f_{pas} \cdot n_{pas}$. f_{pas} is the carbon dioxide amount given off per passenger.

The following substitution is used to simplifies the calculation in Section 3.2.1

$$\Delta h_{SUP} = \dot{m}_{SUP} \cdot c_{air} \cdot (T_{SUP} - T_{IDA}), \tag{4a}$$

$$\Delta \sigma_{SUP} = \dot{m}_{SUP} \cdot (\sigma_{SUP} - \sigma_{IDA}). \tag{4b}$$

Resulting state variable x, control variable u and disturbance v are

$$x = \begin{bmatrix} T_{IDA} \\ T_{veh} \\ \sigma_{IDA} \end{bmatrix}, \quad u = \begin{bmatrix} \Delta h_{SUP} \\ \Delta \sigma_{SUP} \end{bmatrix} \text{and } v = \begin{bmatrix} T_{ODA} \\ n_{pas} \\ \dot{q}_{sol} \end{bmatrix}. \tag{5}$$

so the state space system can be developed.

2.1.2. State space representation

The state space representation of a continuous system is

$$\frac{dx}{dt} = \mathbf{A}(t)x(t) + \mathbf{B}u(t) + \mathbf{E}v(t) \tag{6a}$$

$$y = \mathbf{C}x(t) + \mathbf{D}u(t). \tag{6b}$$

If the Eq. (2a)–(3), are reformulated to a state space representation (see Eq. (6a)) and state, control and disturbance variables are used according to Eq. (5), the matrices

$$\mathbf{A} = \begin{bmatrix} -\frac{k_{IDA} - k_{veh}}{C_{IDA}} & \frac{k_{veh}}{C_{IDA}} & 0 \\ \frac{k_{veh}}{C_{veh}} & -\frac{k_{veh}}{C_{veh}} & 0 \\ 0 & 0 & 0 \end{bmatrix}, \quad \mathbf{B} = \begin{bmatrix} \frac{1}{C_{IDA}} & 0 \\ 0 & 0 \\ 0 & 0 \\ 0 & \frac{1}{V_{IDA} \cdot \rho_{IDA}} \\ 0 & \end{bmatrix} \tag{7a}$$

$$\text{and } \mathbf{E} = \begin{bmatrix} \frac{k_{IDA}}{C_{IDA}} & \frac{k_{pas}}{C_{IDA}} & \frac{k_{sol}}{C_{IDA}} \\ 0 & 0 & 0 \\ 0 & \frac{f_{pas}}{V_{IDA} \cdot \rho_{IDA}} & 0 \end{bmatrix} \tag{7b}$$

are obtained. Further, $y = x$ applies, so $\mathbf{C} = \mathbf{1}$ and $\mathbf{D} = 0$ follow.

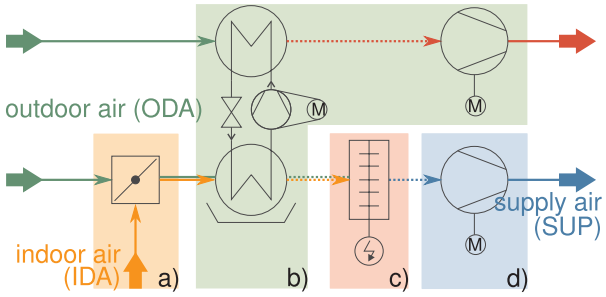

Fig. 3. Sketch of the HVAC; main parts are: (a) mixing chamber (orange background), (b) CRM (green), (c) electric heater (red) and (d) supply air fan (blue). (For interpretation of the references to colour in this figure legend, the reader is referred to the web version of this article.)

2.2. HVAC

The HVAC's purpose is to supply conditioned air (supply air) to the train, for which it consumes electrical energy.

So, relevant outputs of the HVAC model are the conditions of the supply air and the power consumption. The supply air conditions comprise the temperature T_{SUP}, the carbon dioxide concentration σ_{SUP} and the mass flow $\dot{m}_{SUP}$.

2.2.1. HVAC model overview

Fig. 3 shows a sketch of the HVAC and its main parts. Outdoor air enters the HVAC and mixes with recirculation air, which consists of indoor air, inside the mixing chamber. The compression refrigeration machine (CRM) cools and dehumidifies the airflow if it works as an air conditioning. The CRM can work either as air conditioning or as a heat pump; its compressor is variable frequency controlled. It is also possible to heat the air by an electric heater, modulated by an insulated-gate bipolar transistor. The supply air fan blows conditioned air (supply air) into the train, which is phase controlled. All HVAC parts can be controlled in a finite set.

2.2.2. Modelling of parts

Mass balances and the energy balances for each part form the basis for the HVAC model. The main parts are: (a) mixing chamber, (b) CRM, (c) electric heater and (d) supply air fan (see Fig. 3).

The **mixing chamber** alters the temperature and the carbon dioxide concentration of the supply air by mixing the recirculation air flow $\dot{m}_{IDA}$ with the outdoor air flow $\dot{m}_{ODA}$ to a supply air flow $\dot{m}_{SUP}$. The mass balance of air is $\dot{m}_{SUP} = \dot{m}_{IDA} + \dot{m}_{ODA}$, but only the ratio of outdoor air φ_{mc}

$$\varphi_{mc} = \frac{\dot{m}_{ODA}}{\dot{m}_{SUP}}. \tag{8}$$

can be altered directly by a ventilation flap. $\dot{m}_{SUP}$ results from the rotational speed of the supply air fan. The power consumption of the mixing chamber P_{mc} is neglected, so $P_{mc} = 0$. If the CRM works as an air conditioning, supply air must only consist of outdoor air ($\varphi_{mc} = 1$).

The CRM will not affect the mass flow of air and carbon dioxide if it works as an air conditioning, but condensing water on the cold heat exchanger surface must be considered.

Subtracting the heat flow removed by the CRM from the enthalpy flow of incoming air results in the enthalpy flow of outgoing air. The HVAC manufacturer provided a look-up table

$$\dot{Q}_{ac} = \dot{Q}_{ac}(T_{ODA}, \dot{m}_{SUP}, \varphi_{comp}) \tag{9}$$

to calculate the removed heat flow $\dot{Q}_{ac}$.

The electrical power consumption is linearised to depend only on the rotational speed of the compressor φ_{comp}, $P_{ac} = f_{ac} \cdot \varphi_{comp}$ applies. f_{ac} is the scaling factor.

The HVAC manufacturer also provided a look-up table

$$\dot{Q}_{hp} = \dot{Q}_{hp}(T_{ODA}, \dot{m}_{SUP}, \varphi_{comp}) \tag{10}$$

to calculate the introduced heat flow $\dot{Q}_{hp}$ if the CRM works as a heat pump. Again, the electrical power consumption for the CRM P_{hp} depends linearly on φ_{comp}, $P_{hp} = f_{hp} \cdot \varphi_{comp}$ applies. f_{hp} is a scaling factor. The heat flow introduced by the electric heater depends linearly on the chosen setting of the electric heater

$$\dot{Q}_{eh} = f_{eh} \cdot \varphi_{eh}. \tag{11}$$

In case of the electric heater, the electrical power consumption P_{eh} is identical to the introduced heat $\dot{Q}_{eh}$ flow $P_{eh} = \dot{Q}_{eh} = f_{eh} \cdot \varphi_{eh}$. f_{eh} is a scaling factor and φ_{eh} is the activation ratio of the electric heater.

The **supply air fan** produces the mass flow of supply air $\dot{m}_{SUP}$. Any waste heat by the fan is neglected.

The equation of the power consumption depends linearly on the supply air mass flow.

2.2.3. Overall HVAC model

The HVAC model allows calculating the supply air conditions and the power consumption from the known control variable of the HVAC. The HVAC control variable is

$$u_{HVAC} = [\mathscr{M}, \varphi_{mc}, \dot{m}_{SUP}, \varphi_{comp}, \varphi_{eh}]^T. \tag{12}$$

$\mathscr{M}$ is the operation mode of the HVAC. $\dot{m}_{SUP}$ is the mass flow of supply air. φ_{mc} is the outdoor air ratio. φ_{comp} is the rotational speed of the compressor of the CRM and φ_{eh} is the activation ratio of the electric heater φ_{eh}. The model is set up according to modes of the HVAC $\mathscr{M}$, irrespective of whether the humidity of the supply air is changed (because of condensation, for example) or not. Condensation does not occur in case of **Ventilating and Heating**. The condition of the supply air (T_{SUP} and σ_{SUP}) can be calculated by solving the energy balance $\dot{E}_{ODA} + \dot{E}_{IDA} + \dot{Q}_{hp} + \dot{Q}_{eh} - \dot{E}_{SUP} = 0$ and the mass balance for carbon dioxide $\dot{m}_{IDA} \cdot \sigma_{IDA} + \dot{m}_{ODA} \cdot \sigma_{ODA} - \dot{m}_{SUP} \cdot \sigma_{SUP} = 0$

$$T_{SUP} = (1-\varphi_{mc}) \cdot T_{IDA} + \varphi_{mc} \cdot T_{ODA} + \frac{\dot{Q}_{hp} + f_{eh} \cdot \varphi_{eh}}{c_{air} \cdot \dot{m}_{SUP}} \text{ and} \tag{13a}$$

$$\sigma_{SUP} = (1-\varphi_{mc}) \cdot \sigma_{IDA} + \varphi_{mc} \cdot \sigma_{ODA}. \tag{13b}$$

where $\dot{Q}_{hp}$ follows from the look-up table $\dot{Q}_{hp}(T_{ODA}, \dot{m}_{SUP}, \varphi_{comp})$ and σ_{ODA} is the outdoor air concentration of carbon dioxide.

In **Cooling and Dehumidifying** $\sigma_{SUP} = \sigma_{ODA}$ applies because of $\varphi_{mc} = 1$. However, the energy balance for the air-condition cannot be solved directly. If relevant terms are inserted into the energy balance $\dot{E}_{ODA} + \dot{Q}_{eh} - \dot{Q}_{ac} - \dot{E}_{SUP} = 0$, equation

$$\dot{m}_{SUP} \, (c_{air} \, T_{ODA} + Y_{ODA} \, c_{vapour} \, T_{ODA} + Y_{ODA} \, \Delta h_V) + \dot{m}_{SUP} \, (c_{air} \, T_{SUP} + Y_{SUP} \, c_{vapour} \, T_{SUP} + Y_{SUP} \, \Delta h_V) - \dot{Q}_{ac} + \dot{Q}_{eh} = 0 \tag{13c}$$

is obtained, in which $\dot{Q}_{ac}$ follows from the look-up table $\dot{Q}_{ac}(T_{ODA}, \dot{m}_{SUP}, \varphi_{comp})$. Y_{ODA} is the absolute humidity of outdoor air and Y_{SUP} is the absolute humidity of supply air. c_{vapour} is the heat capacity of vapour and Δh_V is the evaporation heat of water. Since there are two unknowns in the equation T_{SUP} and Y_{SUP}, an extra condition needs to be found. It is assumed that the mass flow before the CRM is split into two flows. One flow enters the CRM and is cooled (and dehumidified) to the given surface temperature of the heat exchanger of the CRM T_{ac}. The other flow is left unchanged. Then both flows are mixed again. The AAC stands for the resulting flow. Now only the ratio of the mass flows β needs to be calculated, then T_{SUP} and Y_{SUP} follow.

So, the following linear system of equations needs to be solved.

$$c_{air} \cdot T_{AAC} + \Delta h_V \cdot Y_{AAC} = c_{air} \cdot T_{ODA} + \Delta h_V \cdot Y_{ODA} - \frac{\dot{Q}_{ac}}{\dot{m}_{ODA}} \tag{15a}$$

$$T_{AAC} - (T_{ODA} - T_{ac}) \cdot \beta = T_{ac} \tag{15b}$$

$$Y_{AAC} - (Y_{ODA} - Y_{ac}) \cdot \beta = Y_{ac} \tag{15c}$$

$$Y_{AAC} = Y_{AAC} \tag{15d}$$

$$-T_{AAC} + T_{SUP} = \frac{\dot{Q}_{eh}}{c_{air} \cdot \dot{m}_{SUP}} \tag{15e}$$

Y_{AAC} and T_{AAC} are the absolute humidity of the air after the air conditioning, respectively the temperature. Y_{AAC} is the humidity ratio at T_{ac} (humidity is 100%).

The **overall power consumption** of the HVAC is the sum of the parts power consumption

$$P_{tot} = P_{fan} + P_{ac} + P_{hp} + P_{eh}. \tag{16}$$

2.3. Thermal comfort

This paper defines, thermal comfort according to today's standards and regulations [28], although more advanced methods exist [32]. The managing company of the tram supplied the set-point of the indoor air (IDA) temperature as a piece-wise linear function of outdoor air (ODA) temperature. If the IDA temperature is below the set-point temperature plus the allowed deviation and above the set-point temperature minus the allowed deviation, the wanted comfort is achieved. The deviation is usually ± 2 °C. Deviations are typically more acceptable, if they deviate toward 20 °C.

Since no maximum carbon dioxide concentration is given in [28], 1000 ppm is chosen as set-point agreeing with [33]. Even though the HVAC can reduce the air humidity, it is deliberately not used. Keeping the changes to the thermal comfort to a minimum allows a better comparison between current and new HVAC. Also, the local climate in Vienna is favourable in this regard.

3. Controller design

This Section designs new controllers based on the developed models of the tram, the HVAC and the defined thermal comfort. First, it introduces the thermal comfort control problem and discusses various problem formulations. Then it designs the controllers and shows their implementation on to an RCPP.

3.1. Control structure

The objective of the control problem of thermal comfort is to achieve a high thermal comfort for the passenger inside the train and to use as little electrical energy operating the HVAC as possible. Since operation of the HVAC needs electrical energy, compare Eq. (16), it is obvious that both objectives contradict each other.

A multi-criteria optimisation problem is an optimisation problem with two or more objectives. Kallrath [34, p. 160f] describes different approaches to solve this problem:

Pre-emptive approach In the pre-emptive approach ranks the objectives. If the electrical energy consumption is prioritised, the lowest energy consumption can be achieved by switching the HVAC off. This solution yields unsatisfying results. Another possibility is to prioritise the thermal comfort and afterwards the electrical energy consumption. This approach is further followed. Note that global optimality in the original sense may be lost when using this approach.

Archimedean approach The Archimedean approach combines both objectives into a new, joint objective by suitable weighting factors. The disadvantage of this approach it that suitable values factors need to be found for these factors.

Pareto approach The ideal solutions for all possible combinations of weighting factors are computed. This results in an (estimated) Pareto-front. The best solution on the Pareto-front may be selected by added criteria (robustness, wear, etc. [35]). This approach is computationally expensive, too expensive for the chosen embedded system and cannot be continued.

3.2. Pre-emptive approach

The overall control problem is split into two sub-problems to facilitates computation. It uses a model predictive controller to control the thermal comfort inside the train by an auxiliary control variable. An integer linear optimisation transforms it in an energy-optimal way into switching commands for the HVAC by an integer linear optimisation.

3.2.1. Model predictive controller

The method of least squares is the basis for model predictive control. The objective J is a (weighted) sum of the squared control error e and the change of the control variable Δu during the moving control horizon τ. The sequence of Δu and e is to be calculated for τ.

Problem formulation In a common MPC formulation the objective of

$$J(\vartheta) = \sum_{\vartheta=0}^{\tau-1} \left[e(\vartheta)^T \mathbf{Q}(\vartheta) e(\vartheta) + \Delta u(\vartheta)^T \mathbf{R}(\vartheta) \Delta u(\vartheta)\right] \tag{17}$$

is used where $\mathbf{Q}$ is the weighting matrix of e and $\mathbf{R}$ is the weighting matrix of Δu. The discrete time index ϑ for $e(\vartheta)$ is given by $\vartheta = 1, ..., \tau$, the discrete time index ϑ for $\Delta u(\vartheta)$ is given by $\vartheta = 0, 1, ..., \tau$ and the quadratic problem is given as

$$\begin{aligned}
&\textit{minimise} \quad J(\vartheta), \qquad \vartheta = 0, ..., \tau{-}1 \\
&\textit{subject to} \quad x(\vartheta+1) = \mathbf{A}(\vartheta)x(\vartheta) + \mathbf{B}u(\vartheta) + \mathbf{E}v(\vartheta), \\
&\qquad y(\vartheta) = \mathbf{C}x(\vartheta) \\
&\qquad e(\vartheta) = w(\vartheta){-}y(\vartheta), \\
&\qquad \Delta u(\vartheta) = u(\vartheta){-}u(\vartheta{-}1), \\
&\qquad x^{\mathrm{lb}}(\vartheta) \leqslant x(\vartheta) \leqslant x^{\mathrm{ub}}(\vartheta), \\
&\qquad e^{\mathrm{lb}}(\vartheta) \leqslant e(\vartheta) \leqslant e^{\mathrm{ub}}(\vartheta), \\
&\qquad u^{\mathrm{lb}}(\vartheta) \leqslant u(\vartheta) \leqslant u^{\mathrm{ub}}(\vartheta), \\
&\qquad \Delta u^{\mathrm{lb}}(\vartheta) \leqslant \Delta u(\vartheta) \leqslant \Delta u^{\mathrm{ub}}(\vartheta)
\end{aligned} \tag{18}$$

Problem reformulation. Eq. (18) shows the state x at the next time instance $(\vartheta + 1)$, the control error and the change of the control variable $\Delta u(\vartheta)$ as

$$x(\vartheta+1) = \mathbf{A}(\vartheta)x(\vartheta) + \mathbf{B}u(\vartheta) + \mathbf{E}v(\vartheta) \tag{19}$$

$$e(\vartheta) = w(\vartheta){-}y(\vartheta) \quad \text{and} \tag{20}$$

$$\Delta u(\vartheta) = u(\vartheta){-}u(\vartheta{-}1). \tag{21}$$

Eq. (21) can be inserted in Eq. (19)

$$x(\vartheta+1) = \mathbf{A}(\vartheta)x(\vartheta) + \mathbf{B}u(\vartheta) + \mathbf{B}\Delta u(\vartheta) + \mathbf{E}v(\vartheta). \tag{22}$$

Shifting Eq. (20) to the next time instance and multiplying it by (-1) gives $-e(\vartheta+1) = -w(\vartheta+1) + x(\vartheta+1)$ and substitutingx(ϑ + 1) in Eq. (22) gives

$$e(\vartheta+1) = \mathbf{A}(\vartheta)x(\vartheta) + \mathbf{B}u(\vartheta) + \mathbf{B}\Delta u(\vartheta) + \mathbf{E}v(\vartheta){-}w(\vartheta+1). \tag{23}$$

Instead of x and u, the augmented state vector $\widetilde{x}$ and the matching augmented control vector $\widetilde{u}$ are used ˜ shows the augmentation

$$\widetilde{x}(\vartheta) = \begin{bmatrix} x(\vartheta) \\ -e(\vartheta) \\ u(\vartheta{-}1) \end{bmatrix} \qquad \widetilde{u}(\vartheta) = [\Delta u]. \tag{24}$$

The augmented matrices $\widetilde{\mathbf{A}}$, $\widetilde{\mathbf{B}}$ and the augmented disturbance vector $\widetilde{v}$ follow from Eqs. 22, 23, 21.

$$\widetilde{\mathbf{A}}(\vartheta) = \begin{bmatrix} \mathbf{A}(\vartheta) & \mathbf{0} & \mathbf{B} \\ \mathbf{A}^{\mathrm{ref}}(\vartheta) & \mathbf{0} & \mathbf{B}^{\mathrm{ref}} \\ \mathbf{0} & \mathbf{0} & \mathbf{I} \end{bmatrix} \qquad \widetilde{\mathbf{B}} = \begin{bmatrix} \mathbf{B} \\ \mathbf{B}^{\mathrm{ref}} \\ \mathbf{I} \end{bmatrix} \tag{25}$$

$$\widetilde{v}(\vartheta) = \begin{bmatrix} \mathbf{E}v(\vartheta) \\ \mathbf{E}v^{\mathrm{ref}}(\vartheta){-}w(\vartheta) \\ 0 \end{bmatrix} \tag{26}$$

$-e(\vartheta)$ is used instead of $e(\vartheta)$ because this way algebraic signs of $\mathbf{A}$ and $\mathbf{A}^{\mathrm{ref}}$ are identical and since it is a quadratic problem, $e(\vartheta)$ is squared anyway. The product $\mathbf{E}v(\vartheta)$ results from multiplying the disturbance matrix $\mathbf{E}$ by the disturbance vector $v(\vartheta)$ known in τ. Eq. (27) is obtained by using Eq. (24) in Eq. (17)

$$\widetilde{J}(\vartheta) = \frac{1}{\tau} \sum_{\vartheta=0}^{\tau-1} \left(\widetilde{x}(\vartheta)^T \widetilde{\mathbf{Q}}(\vartheta) \widetilde{x}(\vartheta) + \widetilde{u}(\vartheta)^T \widetilde{\mathbf{R}}(\vartheta) \widetilde{u}(\vartheta)\right), \tag{27}$$

where $\widetilde{\mathbf{Q}}(\vartheta)$ and $\widetilde{\mathbf{R}}(\vartheta)$ are positive semi-definite and

$$\widetilde{\mathbf{Q}}(\vartheta) = \begin{bmatrix} \mathbf{0} & \mathbf{0} & \mathbf{0} \\ \mathbf{0} & \mathbf{Q}(\vartheta) & \mathbf{0} \\ \mathbf{0} & \mathbf{0} & \mathbf{0} \end{bmatrix} \quad \text{and} \quad \widetilde{\mathbf{R}}(\vartheta) = \mathbf{R}(\vartheta) \tag{28}$$

The constraints in $\widetilde{x}(\vartheta)$ and $\widetilde{u}(\vartheta)$

$$\widetilde{x}^{\mathrm{lb}}(\vartheta) \leqslant \widetilde{x} \quad (\vartheta) \leqslant \widetilde{x}^{\mathrm{ub}}(\vartheta), \quad \vartheta = 1, ..., \tau \tag{29}$$

$$\widetilde{u}^{\mathrm{lb}}(\vartheta) \leqslant \widetilde{u} \quad (\vartheta) \leqslant \widetilde{u}^{\mathrm{ub}}(\vartheta), \quad \vartheta = 0, 1, ..., \tau \tag{30}$$

can be written as linear inequalities

$$\mathbf{G_1}\widetilde{x}(\vartheta) + \mathbf{G_2}\widetilde{u}(\vartheta) \leqslant g(\vartheta), \quad \vartheta = 0, 1, ..., \tau \tag{31}$$

and the reformulated quadratic problem is

$$\begin{aligned}
&\textit{minimise} \quad \widetilde{J}(\vartheta), \qquad \vartheta = 0, ..., \tau{-}1 \\
&\textit{subject to} \quad \widetilde{x}(\vartheta+1) = \widetilde{\mathbf{A}}(\vartheta)\widetilde{x}(\vartheta) + \widetilde{\mathbf{B}}\widetilde{u}(\vartheta) + \widetilde{v}(\vartheta) \\
&\qquad \mathbf{G_1}\widetilde{x}(\vartheta) + \mathbf{G_2}\widetilde{u}(\vartheta) \leqslant g
\end{aligned} \tag{32}$$

in the variables

$$x(1), ..., x(\tau) \tag{33}$$

$$u(0), ..., u(\tau{-}1) \tag{34}$$

and parameters

$$\widetilde{x}(0), \widetilde{\mathbf{A}}(\vartheta), \widetilde{\mathbf{B}}, \widetilde{v}(\vartheta), \widetilde{\mathbf{Q}}(\vartheta), \widetilde{\mathbf{R}}(\vartheta), \mathbf{G_1}(\vartheta), \mathbf{G_2}(\vartheta), g(\vartheta), \tag{35}$$

in every time instance ϑ [36].

Solution Procedure The solution procedure proposed by Wang et al. [36] uses a primal barrier interior-point method to solve the quadratic program. They implemented the procedure under a free licence in C code and documented it well. All this simplifies porting the code to an RCPP later.

3.2.2. HVAC Controller

The HVAC model is a linear system and some of its variables are integer. So, it is a (mixed) integer linear problem. A program library, like `lpsolve` [37], solves such a problem. However, porting such a library on to an RCPP is out of scope and is not pursued further.

Instead, a **problem-specific heuristic** is developed.

HVACs mode. Defines the status of each part of the HVAC. Table 1 lists for each mode which variables are control variables (cv), which are off (off) or set to a specific value (min) or (max).

Selection of the HVAC mode. Each mode is represented by its vertices in a $P_{\mathrm{tot}} - \Delta h_{\mathrm{SUP}}$ diagram. The supplied enthalpy (minimum and maximum supplied enthalpy) and the outdoor airflow (minimum and maximum outdoor airflow) are varied, which results in four vertices $\mathscr{P}$

Table 1
Outline of the different HVAC modes and control variables, listing which variables are control variables (cv), which are off (off) or set to a specific value (min) or (max).

Mode	Symb.	φ_{comp}	$\dot{m}_{\mathrm{SUP}}$	φ_{mc}	φ_{eh}
Cooling	$\mathscr{C}$	cv	cv	off	off
Dehumidification	$\mathscr{D}$	min	cv	off	cv
Heating CRM	$\mathscr{H}$	cv	cv	cv	off
Heating el	$\mathscr{E}$	off	cv	cv	cv
Heating el + CRM	$\mathscr{B}$	max	cv	cv	cv
Ventilation	$\mathscr{V}$	off	cv	cv	off

for each mode. $\mathscr{P}_1$ is the minimum supplied enthalpy and minimum outdoor airflow in each mode. $\mathscr{P}_2$ is the minimum supplied enthalpy with the maximum outdoor airflow. $\mathscr{P}_3$ is the maximum supplied enthalpy with the minimum outdoor airflow and $\mathscr{P}_4$ is the maximum supplied enthalpy with the maximum outdoor airflow. In *ventilation* both points $\mathscr{P}_1$ and $\mathscr{P}_4$ respectively $\mathscr{P}_2$ and $\mathscr{P}_3$ overlap one other. Connecting the points results in a rectangle in all other modes ($\overline{\mathscr{P}_2\mathscr{P}_1}$, $\overline{\mathscr{P}_1\mathscr{P}_4}$ and $\overline{\mathscr{P}_4\mathscr{P}_3}$).

Fig. 4 shows that $\mathscr{E}$ provides a smaller power consumption than $\mathscr{V}$ for a given enthalpy set-point $\Delta h_{\mathrm{SUP}}^{\mathrm{ref}}$. A black solid line shows the lowest power consumption from which the HVAC modes follows.

Calculation of the manipulated variables of the HVAC. The heuristic converts the set-point of the master controller into the discrete switching modes of the HVAC u_{HVAC}. Depending on the chosen mode, different algorithms are used, in which the basic idea remains the same. Algorithm 1 shows a pseudo code for the heuristic.

Algorithm 1. Pseudo code of the heuristic

procedure HEURISTIC
  for all $\dot{m}_{\mathrm{ODA}}$ **from** $\dot{m}_{\mathrm{ODA}}^{\mathrm{lb}}$ **to** $\dot{m}_{\mathrm{ODA}}^{\mathrm{ub}}$ **do**
    for all $\dot{m}_{\mathrm{IDA}}$ **from** $\dot{m}_{\mathrm{IDA}}^{\mathrm{lb}}$ **to** $\dot{m}_{\mathrm{IDA}}^{\mathrm{ub}}$ **do**
      $\dot{m}_{\mathrm{SUP}} = \dot{m}_{\mathrm{ODA}} + \dot{m}_{\mathrm{IDA}}$
      $\varphi_{\mathrm{mc}} = \frac{\dot{m}_{\mathrm{ODA}}}{\dot{m}_{\mathrm{SUP}}}$
      if $\dot{m}_{\mathrm{SUP}} \geqslant \dot{m}_{\mathrm{SUP}}^{\mathrm{ub}}$ **then**
        continue
      $T_{\mathrm{SUP}}^{\mathrm{est}} \leftarrow \frac{\Delta h_{\mathrm{SUP}}}{\dot{m}_{\mathrm{SUP}} \cdot c_{\mathrm{air}}} + T_{\mathrm{IDA}}$
      if $\neg(T_{\mathrm{SUP}}^{\mathrm{lb}} \leqslant T_{\mathrm{SUP}}^{\mathrm{est}} \leqslant T_{\mathrm{SUP}}^{\mathrm{ub}})$ **then**
        continue
      Select φ_{comp} or φ_{eh}
      for all $\varphi_{\mathrm{comp/eh}}$ **from** $\varphi_{\mathrm{comp/eh}}^{\mathrm{down}}$ **to** $\varphi_{\mathrm{comp/eh}}^{\mathrm{up}}$ **do**
        calculate P_{tot}
        calculate T_{SUP}, Δh_{SUP}
        if $\neg(T_{\mathrm{SUP}}^{\mathrm{lb}} \leqslant T_{\mathrm{SUP}} \leqslant T_{\mathrm{SUP}}^{\mathrm{ub}})$ **then**
          continue
      min $J \rightarrow P_{\mathrm{tot}}$, Δh_{SUP}

The heuristic iterates over the outdoor airflow from the minimum to the maximum value ($\dot{m}_{\mathrm{ODA}}^{\mathrm{lb}}$ respectively $\dot{m}_{\mathrm{ODA}}^{\mathrm{ub}}$); and then, if available, over the recirculation airflow ($\dot{m}_{\mathrm{IDA}}^{\mathrm{lb}}$ respectively $\dot{m}_{\mathrm{IDA}}^{\mathrm{ub}}$). With the given supply airflow, the supply air temperature is estimated and checked whether the constraints hold. Usually, the remaining manipulated variables (φ_{comp} or φ_{eh}, depending on the mode and skipped during ventilation) can be estimated, and by rounding up or down one gets the wanted switching conditions u_{HVAC}.

For all these possibilities the energy consumption, the supply air conditions and the supplied enthalpy are calculated. Calculating a switching condition stops as early as possible to waste as little computation time as possible with infeasible solutions. If constraints do not hold, a switching possibility is infeasible. The solution with the lowest energy consumption P_{tot} and a small difference to the set-point $\Delta h_{\mathrm{SUP}}^{\mathrm{ref}}$ is selected from all valid solutions. An algorithm solves the (unconstrained) optimisation problem

$$\min_i J = h_{\mathrm{MILP}}(i) + (\Delta h_{\mathrm{SUP}}^{\mathrm{ref}}(i) - \Delta h_{\mathrm{SUP}})^2 \tag{36}$$

in i, in which i is the index of the switching possibilities calculated before.

3.3. Archimedean approach

To prevent occurring unwanted modes (like *dehumidification* and *heating (el)*), the control problem is simplified (by switching to neighbouring modes (*cooling* and *ventilating* respectively *ventilating* and *heating (CRM)*)). Again, various constraints have to be taken into account. A conventional approach for this behaviour could be achieved by a 2-point controller with hysteresis. This work uses an MPC based method that allows considering the various constraints.

Objective. Fig. 4 shows that there are two possibilities to replace the *dehumidification*, either by choosing *cooling* or *ventilation*. In both cases, the thermal comfort decreases because the HVAC supplies either too much or too little enthalpy. The same applies to *heating (el)*, the neighbouring modes are *ventilation* and *heating (CRM)*.

A sequence of the control variable is to be found over the horizon τ that satisfies the thermal comfort constraints. There are only two possibilities for the control variable u, that is $u \in [u_1, u_2]$.

Optimisation problem. The optimisation problem can be written as MPC problem:

$$\begin{aligned} \text{minimise} \quad & \sum_{\vartheta=1}^{\tau} (w(\vartheta) - x(\vartheta))^2 \\ \text{subject to} \quad & x(\vartheta+1) = \mathbf{A}(\vartheta)x(\vartheta) + \mathbf{B}u(\vartheta) + \mathbf{E}v(\vartheta) \\ & x^{\mathrm{lb}}(\vartheta) \leqslant x(\vartheta) \leqslant x^{\mathrm{ub}}(\vartheta), \qquad u \in [u_1, u_2]. \end{aligned} \tag{37}$$

3.4. Implementation

This work uses the Micro Autobox II from dSpace as RCPP. It is integrated into a water-resistant box (see Fig. 5c) and mounted on the tail of the tram (see Fig. 5a and b). The tram provides the power for the Autobox. Data connection is achieved via controller area network bus between the Autobox and the HVACs. The first HVAC serves as the bus master. Due to safety concerns, there is no direct data connection between the Autobox and the tram. Instead, the HVACs and the Autobox form a controller area network (CAN). The first HVAC serves as the bus master. It reads certain data from the tram's multi-function vehicle bus and relays them to the Autobox. A sensor box contains more sensors (GPS and solar radiation). Both communicate via a serial port with the Autobox, which also powers them.

All controllers are set up in Matlab m-code, except for the MPC problem which is already in C and because of speed. A time out watchdog allows the controller area network bus master to detect the absence of the Autobox (for example a software crash on the Autobox crashes) and to switch to a safe mode. Then the HVACs use the current control scheme and cannot use the air conditioning or the heat pump.

4. Results

The tram was transported to the CWT in Vienna. The testing institute contains two climatic wind tunnels, in which the larger one has a test section of 100 m and the smaller one a test section of about 34 m in length. The larger one allows wind speeds of up to 300 km/h, and the maximum wind speed of the smaller wind tunnel is 120 km/h, more than enough for tram tests. Both tunnels allow solar simulation from 250 W/m^2 to 1000 W/m^2, a temperature range of −45 °C to +60 °C

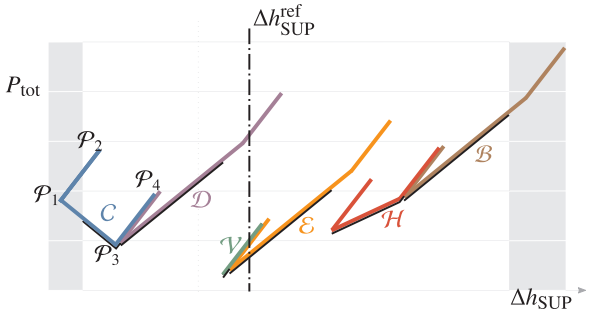

Fig. 4. Selection of the HVAC mode.

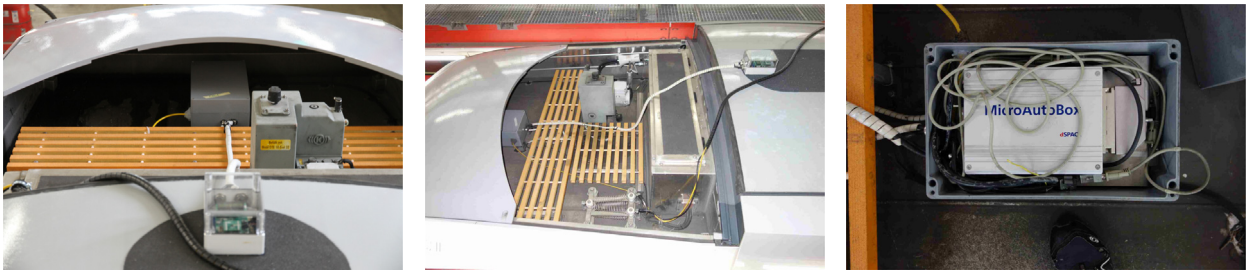

(a) View of the RCPP. In the foreground the box with the solar sensor and the GPS is visible. © A. Fleck

(b) Side view of the RCPP. The RCPP is on the left and the sensor box on the right.

(c) Installation of the RCPP

Fig. 5. Integration of the rapid controller prototyping platform (RCPP).

and a humidity range of 10–98%. [38].

The CWT's team equipped the tram with several temperature, humidity, and energy sensors as well as load simulators during preparation. The tram underwent many experiments confirming the overall system (tram, HVAC, and controller) during a twelve-day measurement campaign.

4.1. Individual tests

This section exemplifies six individual tests, four stationary tests and two dynamic tests. Usually, much effort is put into testing the HVAC's limits that are agreed by contract. However, these limits hardly occur in daily operation. The presented energy-saving HVAC needs a different approach.

It is known from pretests that the HVAC works between its limits (−20 °C to 35 °C). Testing focuses on the most frequent operating conditions. These conditions depend on the city, the train and on how it is operated. They cannot be generalized and must be specifically determined for other use cases.

The test schedule contains the following temperatures:

(a) −10 °C
A winter day in Vienna can be as cold as −10 °C. The service time of the tram starts at 4:30 and ends at 0:30. The tram is hardly occupied at these times and due to building's shade there is almost no irradiation. The HVAC should use Heating (el) to temper the tram.

(b) 5 °C
This test shows the off-peak hours of a spring or autumn day. 5 °C is also the lowest temperature at which the heat pump can be used reasonably. The HVAC should use Heating (CRM) to temper the tram.

(c) 20 °C
Conditions of a spring or autumn day are tested here. 20 °C is the most common outdoor air temperature. The average number of passengers is 42. (All seats are taken). The HVAC should just use Ventilation or Cooling. Dehumidification should be avoided.

(d) 28 °C
These are the conditions of a summer day with the average number of passengers in the tram.

(e,f) 0–28 °C respectively 28–0 °C
Show (almost) the complete operating range of the HVAC in a short testing time. The HVAC should choose the correct HVAC mode over the entire range.

Table 2 shows environmental conditions of the conducted tests and the resulting energy consumption. Fig. 1 shows the IDA temperature time series against the test time for each test. Besides the mean temperature T_{IDA}, it also shows the minimum and the maximum temperatures (T^{-}_{IDA} respectively T^{+}_{IDA}) at different measuring positions of the tram. The temperature range that satisfies the thermal comfort has a white background, everything else has a grey background. The shown signals are temperature measurements of the CWT. Measurements from the HVAC used for control are not available. This phenomenon shows the problem of inhomogeneous temperature distribution in the passenger compartment.

In addition, the power consumption of the individual parts (fan, compressor, and electric heater) as well as the overall power

Table 2
Environmental conditions of the conducted tests and the resulting energy consumption.

No.		Inputs			Results					Results are plotted as bar charts
		T_{ODA} °C	Load Pers.	Sun W/m²	P_{fan} kW[1]	P_{eh} kW[1]	P_{comp} kW[1]	P_{tot} kW[1]	Saving %	P_{fan} P_{eh} P_{comp} 0 1 2 3 4 5 6 kW h/h 8
a	current	−10	0	0	0.84	6.89	0	7.79	—	
	new	−10	0	0	0.57	6.57	0	7.14	9	
b	current	5	0	0	0.90	2.98	0	3.88	–	
	new	5	0	0	1.07	0	1.57	2.64	32	
c	current	20	42	0	1.13	0.03	1.70	2.86	–	
	new	20	42	0	1.45	0	0.97	2.42	15	
d	current	28	42	0	1.21	0.01	2.81	4.03	–	
	new	28	42	0	1.12	0	2.62	3.82	5	
e	current	0 – 28	0	0	0.90	1.27	0.26	2.43	–	
	new	0 – 28	0	0	0.85	0.43	0.81	2.09	14	
f	current	28 – 0	0	700	0.94	1.05	0.88	2.87	–	
	new	28 – 0	0	700	0.82	0.26	0.92	1.99	31	

[1] Energy consumption of the parts as mean value over one hour in kWh/h.

consumption are listed as hourly mean energy consumption in kW h/h for every test. Reference values are taken from measurements conducted on the same vehicle without modifications two years earlier. Results are presented graphically and tabularly (Table 2).

a

Fig. 6a shows the mean IDA temperature varying by 1.5 °C just above the limit. Only for short periods, the mean temperature is below the limit. The IDA range is moderate with 2 °C to 3 °C. The pre-emptive controller can take advantage of the fine-grained control possibilities, which allows the supply air fan to reduce the mass flow. The total energy consumption is reduced by 9% or 0.65 kW h/h.

b

The used Archimedean controller successfully suppresses *Heating (el)* by switching between *Heating (CRM)* and *Ventilation* modes. It achieves an acceptable mean temperature and an energy saving of 32% or 1.24kW h/h. However, the temperature varies by 4 °C in 20 min, which might be unpleasant for the passengers (see Fig. 6b). More over, the IDA temperature range increases rapidly from (almost) zero to 3 °C in 20 min.

c

The Archimedean controller successfully suppresses *Dehumidification* by switching between *Cooling* and *Ventilation*. The achieved mean temperature is acceptable and during alternating the temperature varies only by 0.7 °C (see Fig. 6c). The mean IDA temperature is stable. T^{+}_{IDA} slowly increases and the difference to the mean IDA also increases. This occurs because the tail section does not have its own HVAC but is supplied by the third HVAC. An energy saving of 15% or 0.44 kW h/h is achieved.

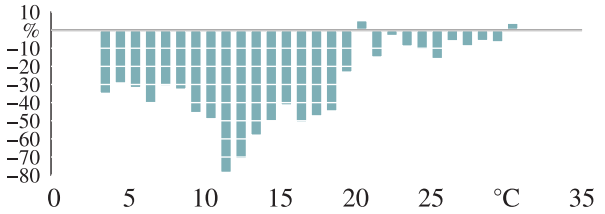

Fig. 7. Relative energy savings of the new tram (compared with the current tram) against the ODA temperature.

d

The energy saving is low with 5% or 0.206 kW h/h, but the HVAC works near its design point during testing. So, no improvement was expected. Fig. 6d shows that the temperature varies by 1.5 °C. The temperature constraints are violated several times, the violation is quite small (0.7 °C). The tail effect described in (c) is present again.

e

The proper controller is always used and switching between both controllers works smoothly. Thermal comfort constraints are satisfied, except during switching between *Heating (CRM)* and *Ventilation* (as seen in No. b). Fig. 6e shows *Heating (el)* during the first hour. The HVAC alternates between *Ventilation* and *Heating (CRM)* for the next four hours. Then the HVAC ventilates for about an hour until it alternates between *Ventilation* and *Cooling*. The achieved energy saving is 14% or 0.332 kW h/h.

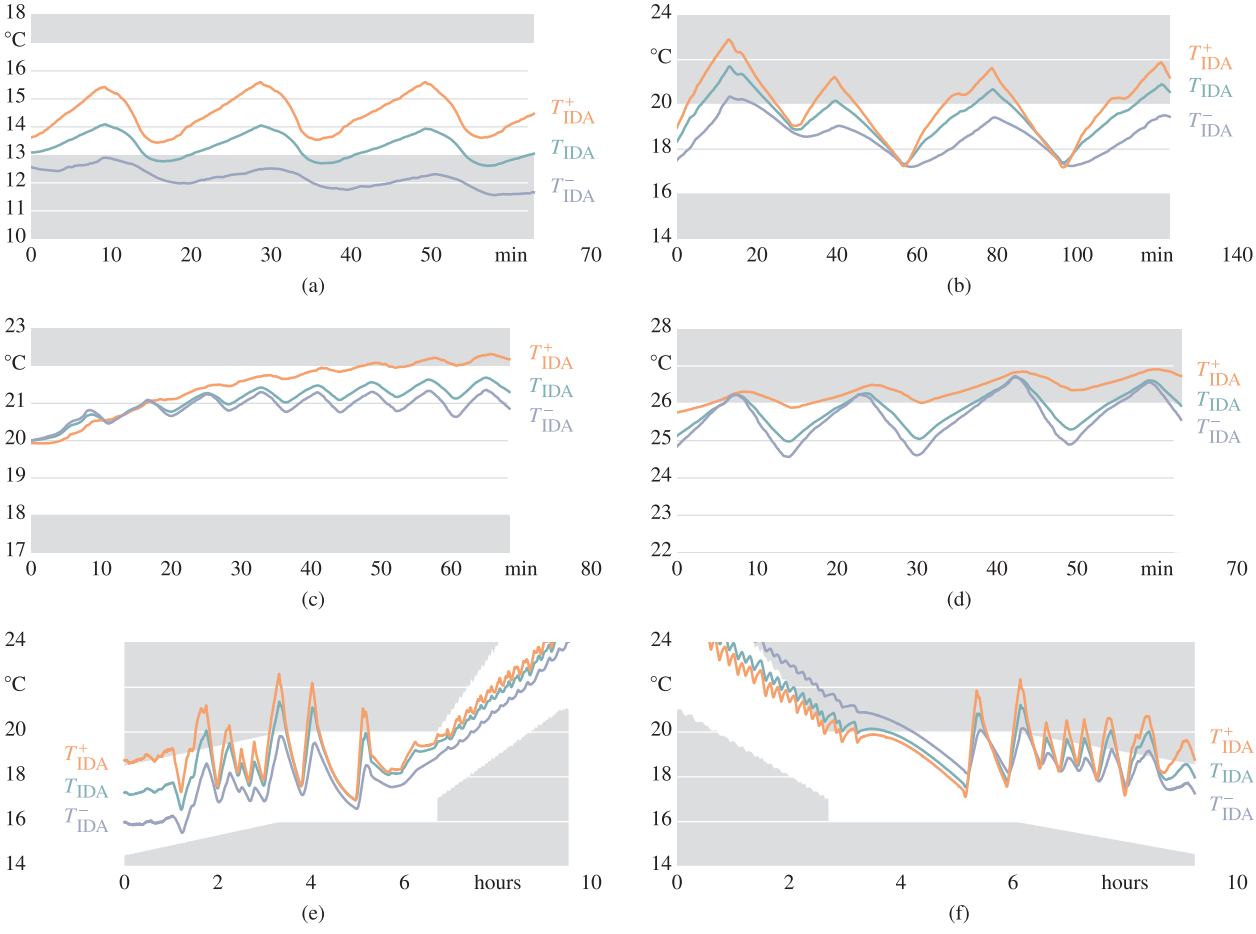

Fig. 6. Time series of the IDA temperature for individual tests.

f

Switching between new controllers works smoothly again. The thermal comfort is near the upper end of the feasible range, but is acceptable. Fig. 6f shows alternating between *Cooling* and *Ventilation*, then a distinctive *Ventilation* phase and again alternating between *Heating (CRM)* and *Ventilation* at the end. There is only a short *Heating (el)* phase in the end. Energy saving is as high as 31% or 0.874 kW h/h.

4.2. Annual energy consumption

Richter [39] proposed a method for calculating the annual energy consumption from individual measurements.

Several temperature ramps (0–28 °C at different solar radiation intensities (0 W/m^2 and 700 W/m^2) and different load levels (0 passengers and 42 passengers) were measured for both tram configurations. For each configuration, a mean power consumption is calculated at every ODA temperature for each experiment. The energy consumption of the current tram is assumed to be 100% at every ODA temperature. Then the relative saving of the new vehicle is calculated. One gets the power consumption of the tram versus the ODA temperature. An overall saving of 32% is achieved for the entire temperature range. Fig. 7 shows the relative energy saving of the new tram compared to the current layout.

5. Conclusions

Transport accounts for much of the overall energy consumption, and the second largest energy consumer in rail vehicles is the HVAC. Energy saving HVACs (including demand-based ventilation, heat pumps and fine-grained control of their parts) need a proper control because of the increased difficulty of the control problem. This paper models for all aspects of the thermal comfort problem in trams (trams, HVAC and thermal comfort) and proposes a controller design of two different approaches. The first approach splits the control problem to facilitate calculation. An MPC controls the tram model and calculates an auxiliary control variable. Then a method based on integer linear optimisation calculates switching commands for the HVAC. The second approach prevents only unwanted conditions using a model predictive control based method. All libraries and algorithms were set up on the dSpace Autobox and built into a tram. The Viennese climatic wind tunnel tested the train during a twelve-day measuring campaign. Individual tests showed savings from 9% to 32% and an estimated annual energy saving of 32%. The research has proved that the proposed approach works well, although, it needs minor adjustments (satisfy constraints and prevent overshooting during the Archimedean approach) for broad application.

Acknowledgements

The project EcoTram (FFG, No. 825 443) supported this work in cooperation with Schieneninfrastruktur-Dienstleistungsgesellschaft m.b.H, Siemens AG Österreich, Vossloh Kiepe Ges.m.b.H, and Wiener Linien GmbH & Co KG. The authors thank the four anonymous reviewers whose comments and suggestions helped to improve and clarify this manuscript.

References

[1] Intergovernmental Panel on Climate Change, Climate Change: The IPCC scientific assessment, Cambridge University Press, Cambridge, Great Britain, 1990 (Ca. 414 pages).
[2] European Commission, EUROPE 2020: A European strategy for smart, sustainable and inclusive growth, Publications Office of the European Union, Brussels, 2010 (EN Version).
[3] U. Maaßen, Energieflussbild 2015 für die Bundesrepublik Deutschland in PJ, Technical Report, AG Energiebilanzen e.V., Berlin Charlottenburg, 2016 (German).
[4] N. Richter, Daten zum Verkehr – Ausgabe 2012, Umweltbundesamt, Postfach 1406, 06813 Dessau, 2012 (German).
[5] W. Knörr, C. Heidt, A. Schacht, Aktualisierung, Daten- und Rechenmodell: Energieverbrauch und Schadstoffemissionen des motorisierten Verkehrs in Deutschland 1960–2030" (TREMOD) für die Emissionsberichterstattung 2013 (Berichtsperiode 1990–2011), Endbericht, FKZ-No. 360 16 037, Umweltbundesamt, Postfach 1406, 06813 Dessau, 2012.
[6] H. Helms, U. Lambrecht, The potential contribution of light weighting to reduce transport energy consumption, Int. J. Life Cycle Assessment 12 (2007) 58–64.
[7] K. Hiller, E. Bunger, E. Firschau, New locomotives for shunting and line operations, Rail Technol. Rev. 52 (2012) 24–28.
[8] W. Struckl, Green Line – Umweltgerechte Produktentwicklungsstrategien für Schienenfahrzeuge auf Basis der Lebenszyklusanalyse des Metrofahrzeuges Oslo (Ph.D thesis), Vienna University of Technology, 2007.
[9] T. Zhang, Q.Y. Chen, Novel air distribution systems for commercial aircraft cabins, Build. Environ. 42 (2007) 1675–1684.
[10] T. Blasse, Rail vehicle with an air-permeable wall for internal ventilation by displacement or source ventilation, 2015 (EP 2868502).
[11] S. Boyd, L. Vandenberghe, Convex Optimization, Cambridge University Press, New York, NY, USA, 2004.
[12] L.F. Larsen, T. Geyer, M. Morari, Hybrid model predictive control in supermarket refrigeration systems, IFAC Proc. Volumes 38 (2005) 313–318.
[13] M.S. Elliott, B.P. Rasmussen, Model-based predictive control of a multi-evaporator vapor compression cooling cycle, American Control Conference, IEEE, 2008, pp. 1463–1468.
[14] G. Bejarano, C. Vivas, M.G. Ortega, M. Vargas, Suboptimal hierarchical control strategy to improve energy efficiency of vapour-compression refrigeration systems, Appl. Therm. Eng. 125 (2017) 165–184.
[15] B. Li, R. Otten, V. Chandan, W.F. Mohs, J. Berge, A.G. Alleyne, Optimal on–off control of refrigerated transport systems, Control Eng. Pract. 18 (2010) 1406–1417.
[16] R. Bourdais, H. Guéguen, Distributed predictive control for complex hybrid system. The refrigeration system example, IFAC Proc. Volumes 43 (2010) 388–394.
[17] T.G. Hovgaard, L.F. Larsen, K. Edlund, J.B. Jørgensen, Model predictive control technologies for efficient and flexible power consumption in refrigeration systems, Energy 44 (2012) 105–116.
[18] M. Killian, B. Mayer, M. Kozek, Hierarchical fuzzy mpc concept for building heating control, IFAC Proc. Volumes 47 (2014) 12048–12055.
[19] B. Mayer, M. Killian, M. Kozek, A branch and bound approach for building cooling supply control with hybrid model predictive control, Energy Buildings 128 (2016) 553–566.
[20] F. Kennel, D. Gorges, S. Liu, Energy management for smart grids with electric vehicles based on hierarchical MPC, IEEE Trans. Ind. Informatics 9 (2013) 1528–1537.
[21] L. Johannesson, M. Asbogard, B. Egardt, Assessing the potential of predictive control for hybrid vehicle powertrains using stochastic dynamic programming, IEEE Trans. Intell. Transp. Syst. 8 (2007) 71–83.
[22] R. Muhammad, M.K. Kamaruddin, Y.P. See, Influence of passenger car air conditioner system thermostat level setting to fuel consumption and thermal comfort, Engineering Applications for New Materials and Technologies, Springer, 2018, pp. 183–195.
[23] J. Kim, S. Schiavon, G. Brager, Personal comfort models–a new paradigm in thermal comfort for occupant-centric environmental control, Building Environ. 132 (2018) 114–124.
[24] D. Kristanto, T. Leephakpreeda, Energy conversion for thermal comfort and air quality within car cabin, IOP Conference Series: Materials Science and Engineering, vol. 187, IOP Publishing, 2017, p. 012037.
[25] F. Bode, I. Nastase, P. Danca, A. Meslem, The influence of the inlet angle of vehicle air diffuser on the thermal comfort of passengers, ENERGY and ENVIRONMENT (CIEM), 2017 International Conference on, IEEE, 2017, pp. 442–446.
[26] A. Velivelli, D. Guerithault, S. Stöwe, Optimum seat cooling distribution for targeted human thermal comfort®, SAE Int. J. Passenger Cars-Mech. Syst. 10 (2017) 128–134.
[27] DIN EN 13129-2:2004-10, Railway applications – Air conditioning for main line rolling stock – Part 2: Type tests, 2004 (German Version).
[28] DIN EN 14750:2006-08, Railway applications – Air conditioning for urban and suburban rolling stock, 2006 (German Version).
[29] R.N. Hofstädter, M. Kozek, Holistic thermal simulation model of a tram, Conference on Computer Modelling and Simulation, Proceedings, Brno, 2011.
[30] C. Dullinger, W. Struckl, M. Kozek, A modular thermal simulation tool for computing energy consumption of HVAC units in rail vehicles, Appl. Therm. Eng. 78 (2015) 616–629.
[31] R.N. Hofstädter, T. Zero, C. Dullinger, G. Richter, M. Kozek, Heat capacity and heat transfer coefficient estimation for a dynamic thermal model of rail vehicles, Math. Comp. Modell. Dynamical Syst. (2016) 1–14.
[32] DIN EN ISO 7730:2005, Ergonomics of the thermal environment - Analytical determination and interpretation of thermal comfort using calculation of the PMV and PPD indices and local thermal comfort criteria, Standard, DIN Deutsches Institut für Normung e. V., Berlin, 2006.
[33] DIN EN 13779:2007-09, Ventilation for non-residential buildings – Performance requirements for ventilation and room-conditioning systems, Standard, DIN Deutsches Institut für Normung e.V., Berlin, 2007 (German version).
[34] J. Kallrath, h jks hfk, Gemischt-ganzzahlige Optimierung: Modellierung in der Praxis: mit Fallstudien aus Chemie, Energiewirtschaft, Metallgewerbe, Produktion und Logistik, Vieweg+ Teubner, Braunschweig u.a., 2002.
[35] E. Luchini, F. Kitanoski, M. Kozek, Multi-objective optimization of the operational modes for redundant refrigeration circuits, Appl. Therm. Eng. 122 (2017) 409–419.
[36] Y. Wang, S. Boyd, Fast model predictive control using online optimization, IEEE Trans. Control Syst. Technol. 18 (2010) 267–278.
[37] M. Berkelaar, K. Eikland, P. Notebaert, Open source (Mixed-Integer) Linear Programming system, 2004 (Version 5.5.2.).
[38] G. Haller, Der neue klima-wind-kanal in wien, in: ZEVrail Glasers Annalen 126, 38. Grazer Schienenfahrzeugtagung, Institute of Railway Engineering and Transport Economy, Graz University of Technology, 2002, pp. 22–27.
[39] G. Richter, Ecotram research project: how much energy is used by the HVAC of a tram? measurements in the climatic wind tunnel and in service, Railvolution 10 (2010).